First-principles calculations for a model Hamiltonian treatment of hybridizing light actinide compounds

John M. Wills
Theoretical Division, Los Alamos National Laboratory, Los Alamos, New Mexico 87544

Bernard R. Cooper
Department of Physics, West Virginia University, Morgantown, West Virginia 26506
and Center for Materials Science, Los Alamos National Laboratory, Los Alamos, New Mexico 87544
(Received 15 March 1989; revised manuscript received 26 February 1990)

A procedure, previously applied to Ce(f^1) systems, for calculating the components of an Anderson-model lattice Hamiltonian has been extended to hybridizing actinide ($f^{n>1}$) systems and applied to some hybridizing Pu compounds with magnetic behavior of great current interest. There are some differences in the treatment of actinide systems compared with cerium systems, arising both from the greater spatial extent of $5f$ states compared with $4f$ states and from the many-electron character of the actinide correlated quasi-ionic states. The band-f hybridization matrix elements and band energies in the Anderson Hamiltonian are obtained from warped-muffin-tin linear muffin-tin-orbital band-structure calculations with Pu $5f$ states treated as "just bound" core-like states. The calculations are performed for PuAs, PuSb, PuBi, and PuTe. Pu $5f$ energy levels, relative to the Fermi energy, are calculated for PuSb from total-energy supercell calculations with four, five, and six electrons in the Pu $5f$ core. We analyze the source in the electronic structure of trends between materials in hybridization-induced effects by considering the behavior of two quantities: (1) f-state resonance widths, characterizing the strength of hybridization, and (2) the density of states at the Fermi energy, characterizing the number and character of band states available for hybridization. Besides assessing the trend in hybridization effects in relationship to changes in the electronic structure between materials, the results are used to evaluate two quantities arising in the model Hamiltonian treatment from hybridization between Pu f states and band states: a shift in the crystal-field levels of the Pu($f^5, J=\frac{5}{2}$) multiplet and a two-ion exchange interaction between Pu ions on different sites. We compare the calculated quantities with experimental results and with previous phenomenological calculations of the magnetic behavior of PuSb, and discuss the implications of our calculations for the magnetic behavior to be expected in these materials. Experimentally, the magnetic behavior of PuSb and PuTe are quite different; so it is interesting that changes in the calculated magnitude and range dependence of the exchange parameters between PuSb and PuTe indicate a qualitative change in the nature of the expected magnetic behavior.

I. INTRODUCTION

In recent years there has been a great deal of activity modeling the behavior of correlated f-electron systems by use of an Anderson-model lattice Hamiltonian. It is of great interest to calculate the parameters of such a Hamiltonian on the basis of *ab initio* electronic structure calculations. This provides both an understanding of the basis, in the underlying electronic structure, for the phenomenological behavior and a means of making the phenomenological calculations predictive (i.e., capable of predicting changes in behavior for different materials). In previous work,[1] we have developed a computational scheme to perform such a first-principles evaluation of parameters for hybridizing cerium (f^1) systems. We have now extended that scheme for actinide ($f^{n>1}$) systems, and use the results of our procedure to analyze the trends between materials in hybridization-induced effects, in relationship to changes in the electronic structure.

There are differences in the treatment of plutonium systems compared with that for cerium systems, arising both from the circumstance that the $5f$ states are spatially more extended than $4f$ states and from the fact that the actinide correlated quasi-ionic state contains several f electrons. The greater spatial extent requires a change in the boundary condition imposed on the $5f$ wave functions to obtain localized states; the changed boundary condition provides "just bound" $5f$ states. For cerium systems with a single $4f$ electron, the f states were treated as fully relativistic $j=\frac{5}{2}$ states; however, for actinide systems such as the plutonium compounds treated here, there are several $5f$ electrons, and the correlated quasi-ionic state formed is closer to the L-S coupled limit than to the j-j coupled limit. Thus to provide an appropriate set of one-electron $5f$ states that can be coupled together to give the many-electron quasi-ionic state, we calculate the one-electron $5f$ states as scalar relativistic states, i.e., spin-orbit effects are omitted when the $5f$ basis states are calculated. Spin-orbit effects for the quasilocalized $5f$ electrons are then included when calculating quantities

pertinent to the quasi-ionic state of the model Hamiltonian.

Our first application of this treatment to actinide systems has been to some hybridizing plutonium compounds, the NaCl-structure plutonium monopnictides and monochalcogenides. The magnetic properties of these Pu compounds are of current interest both experimentally and theoretically.[2] The Pu monopnictides exhibit a variety of magnetic structures, characterized by a strong anisotropy with moments lying along a cube edge.[3] The behavior of PuSb, and the contrast on going to PuTe, is of particular interest. PuSb has[3] a transition to long period antiferromagnetic order at a Néel temperature of 85 K and a transition to ferromagnetic behavior at 67 K.[2] The magnetic excitation behavior is also highly unusual showing peculiar dispersion and polarization.[4] In sharp contrast to the behavior of PuSb, the chalcogenide PuTe is an enhanced paramagnet.[5]

The magnetic behavior of PuSb is similar in complexity to that of CeSb, which can be understood[6] in detail on the basis of a two-ion anisotropic exchange interaction arising from hybridization between band states and f states. The applicable model Hamiltonian is obtained by application of the Schrieffer-Wolff transformation to the Anderson Hamiltonian.[7,8] The similarity between the ground states of the Ce and Pu ions and the fact[9] that these two ions are where the delocalization of the f electrons begins to occur for a given isostructural compound on coming from the heavy end of the rare earths and actinides, respectively, suggests that the physics of the magnetic behavior of Pu compounds may be similar to that of corresponding Ce compounds.[6] An application of the extension of the phenomenological (model Hamiltonian) theory to Pu systems,[10] has proved successful in explaining the magnetic ordering of PuSb and in explaining and predicting many of the features of the magnetic excitation spectrum of that compound.[11–13] The model Hamiltonian parameters in this treatment have been considered to be phenomenological input.

The model Hamiltonian theory of the magnetic behavior of Pu compounds is considerably more complicated than the corresponding theory for Ce compounds. A reasonable description of the magnetic ordering and excitation behavior of PuSb requires a careful treatment of the many-body character of the ground state of the Pu ion,[11–13] introducing an additional set of parameters into the phenomenological treatment to model the contributions of a hierarchy of resonant scattering channels.[13] The strong crystal field in PuSb (reversed in sign relative to that expected from the usual point-charge model[11,14]) introduces an additional sensitivity into the phenomenological calculations.[13] The sensitivity of the predictions of the theory to the interplay between the parameters entering the model Hamiltonian calculations complicates both the task of understanding the detailed physics of these systems and the application of the model Hamiltonian theory to the prediction of the magnetic behavior of materials where experimental observations are lacking. Hence a first-principles analysis of the model Hamiltonian parameters arising from the band-f hybridization interaction is highly desirable as a guide to understanding the behavior of PuSb and in predicting the magnetic behavior of similar Pu compounds.

We have previously reported a calculation of the parameters entering the model Hamiltonian theory for Ce monopnictides.[1] In this paper we report the results of similar calculations applied to the Pu monopnictides PuAs, PuSb, and PuBi, and the monochalcogenide PuTe. The basic quantities required are the parameters of the Anderson Hamiltonian for f-electron materials: band energies ε_k, band-f matrix elements V_{kf}, and the f-state energy levels E_f and E_f+U. Band energies are obtained from self-consistent warped-muffin-tin linear muffin-tin-orbital (LMTO) band-structure calculations, with Pu f states treated (self-consistently) as core states, neglecting band-f hybridization. The potential, band eigenvectors, and Pu f-state wave functions resulting from the self-consistent band calculations are used to obtain the band-f hybridization matrix elements between non-f band states and Pu f states as the matrix elements of the potential surrounding a Pu site, projecting out band-f nonorthogonality.[1] The f-state energies E_f (the energy necessary to remove an f electron from the Pu f^5 multiplet and place it in a band state at the Fermi energy) and E_f+U (the energy necessary to add an electron to the f^5 multiplet from a band state at the Fermi energy) are obtained from supercell calculations for PuSb; similar calculations have been previously performed for Ce compounds.[15]

Our primary motivation in performing these calculations is to evaluate the utility and limitations of the procedure described above as a method for providing first-principles input into Anderson model Hamiltonian calculations for these f^5 systems. For this purpose, we use the calculated parameters to evaluate two specific quantities arising in the model Hamiltonian description of these Pu compounds: a shift in the crystal-field levels of the Pu ground-state manifold due to band-f hybridization,[1,8] and the coefficients ("range parameters") of the exchange interaction between Pu ions, mediated by band electrons, the source of the unusual magnetic ordering and excitation behavior of PuSb.[11–12] Our focus is on testing the utility of the methodology for predicting and understanding the systematics of changes and similarities in hybridization-dominated observational behavior associated with changes in the underlying electronic structure and degree of f-electron delocalization. For this reason we focus our attention on the systematics of changes of behavior for isostructural materials, e.g., on changes going down the pnictogen column for the plutonium monopnictides or on going from a monopnictide to the corresponding monochalcogenide (e.g., antimonide to telluride), and on the changes from a cerium compound to the corresponding plutonium compound.

The results of our calculations for PuSb are compared with experiment and with phenomenological parameters used in the model Hamiltonian calculations for this material. The sign of the crystal-field splitting of the Pu $5f$ $J=\frac{5}{2}$ manifold in PuSb is opposite to that expected on the basis of a point-charge crystal-field model, with the Γ_8 quartet falling substantially below the Γ_7 doublet.[11–13,14] In the Ce monopnictides, band-f hybridiza-

tion causes a considerable reduction in the splitting of the Ce f-state crystal-field levels,[1] and it was predicted on the basis of the model Hamiltonian calculations of the magnetically ordered states in PuSb that the sign of the crystal-field splitting would be reversed from that expected on the basis of the point-charge model.[11] This prediction was subsequently supported experimentally.[14] Our present calculations are performed for the ${}^6H_{5/2}$ Hund's rule state, which is close to the true ground state of the Pu ion, and we find a strong lowering of the Γ_8 level relative to the Γ_7 level, due to band-f hybridization, for this state.

A second test of the calculated parameters is obtained by comparing range parameters calculated for PuSb with phenomenological parameters fitted to the magnetically ordered states of that compound. These range parameters are the coefficients of one-electron transitions in the effective exchange interaction between Pu ions induced by band-f hybridization [see Eq. (2.3)], and the relative signs and magnitudes of these coefficients determine the transition temperatures and character of the magnetically ordered states. The set of phenomenological range parameters is restricted, by an asymptotic condition,[7] to a single parameter for each neighbor shell, and for this reason the comparison between calculated parameters, comprising a full 14×14 matrix for each neighbor, and the phenomenological parameters is not precise, and in this paper we will simply compare the signs and magnitudes of the corresponding components of the calculated and phenomenological range parameters, and appraise the validity of the asymptotic condition imposed in the phenomenological treatment.

After comparing the quantities calculated for PuSb with experiment and phenomenology, we present results for the neighboring monopnictides PuAs and PuBi, and the chalcogenide PuTe, and discuss the differences in magnetic behavior to be expected on the basis of the trends in the calculated parameters. The differences among the Pu monopnictides are relatively subtle; the difference in the calculated parameters between PuSb and PuTe are striking.

In Sec. II we give a brief description of the terms in the model Hamiltonian giving rise to the crystal-field dressing and the two-ion exchange interaction. A detailed description of the model Hamiltonian and the extension to Pu systems may be found in Refs. 1, 6, 8, and 10. In Sec. III we outline the calculation of the model Hamiltonian parameters for Pu systems, pointing out similarities and differences in the calculations compared to those previously reported for the Ce monopnictides.[1] In Sec. IV we present results of calculations of the crystal-field dressing and range parameters for PuAs, PuBi, PuSb, and PuTe, comparing calculated parameters for PuSb with experiment and phenomenology, and discussing the trends in the calculated parameters between the various compounds. In Sec. V we give a summary and a discussion of further applications of this work.

II. THE MODEL HAMILTONIAN FOR PU SYSTEMS

The part of the model Hamiltonian arising from hybridization between band states and Pu $5f$ states is based on a Hamiltonian obtained from the Anderson Hamiltonian by application of the Schrieffer-Wolff transformation.[16] The main result of the transformation is to replace the band-f hybridization term, H_1 in the Anderson Hamiltonian, by terms of second and higher order in H_1. The lowest-order term is of second order and arises directly from the Schrieffer-Wolff transformation.[17] This term takes the form[1]

$$H_2=\sum_{ij}\sum_{k}J_{ij}(k)c_i^{\dagger}c_j \tag{2.1}$$

with $J_{ij}(k)$ given by[1]

$$J_{ij}(k)=-V_{ki}^{*}V_{kj}\left[\frac{\Theta(\varepsilon_k-E_F)}{\varepsilon_k-E_f}+\frac{\Theta(E_F-\varepsilon_k)}{\varepsilon_k-E_f-U}\right], \tag{2.2}$$

where the V_{ki} are the band-f hybridization matrix elements in the Anderson Hamiltonian and the ε_k are band energies. E_f and E_f+U are the energies, ignoring multiplet splitting, to remove an electron from or add an electron to the f-electron ground state of the unhybridized system. The one-electron creation and annihilation operators in Eqs. (2.1) and (2.2) are referenced to the basis set appropriate to the system being studied. For Ce systems, the indices i and j in Eqs. (2.1) and (2.2) refer to the six elements $|m_j\rangle$ of the Ce $4f_{5/2}$ manifold; for Pu systems, the indices refer to the fourteen elements $|m_l m_s\rangle$ of the Pu $5f$ manifold.

H_2 [Eq. (2.1)], has the symmetry of the unhybridized system (cubic symmetry for the Pu compounds considered here) and may be considered as a shift in the f-state crystal-field levels of the unhybridized system. For Ce (f^1) systems, these shifts are the one-electron eigenvalues of H_2 evaluated in the Ce $4f_{5/2}$ basis; the magnitude and sign of the energy shifts depends on the magnitude and character (anion p, Ce d) of the density of band states near the Fermi energy and on the degeneracy of the bands as related by space group symmetry.[1] In Pu (f^5) systems, the shifts in the crystal-field energies are obtained by diagonalizing H_2 in a basis composed of the crystal-field states of the f^5 ($J=\frac{5}{2}$) ground-state multiplet of the Pu ion, and the sign and magnitude of the shifts will depend on the composition of the ground-state multiplet as well as on the one-electron eigenvalues of H_2. In Sec. IV we will examine the five-electron eigenvalues of the second-order Hamiltonian H_2 in two limiting cases for the Pu ground state, the j-j–coupled limit, and the more physically appropriate L-S–coupled (Hund's rule) limit.

The other term in the model Hamiltonian arising from band-f hybridization is of fourth order in H_1, and takes the form of an effective two-ion anisotropic exchange interaction between f states on different ions. This term in the Hamiltonian results from combining perturbation theory on second-order terms with fourth-order terms arising from the Schrieffer-Wolff transformation. The exchange interaction between ions at sites $\mathbf{R}_1$ and $\mathbf{R}_2$ takes the form[1]

$$H_{12} = -\sum_{ij} E_{ij}(\mathbf{R}_1 - \mathbf{R}_2) c_i^{\dagger}(1) c_j(1) c_j^{\dagger}(2) c_i(2) \qquad (2.3)$$

with range functions $E_{ij}(\mathbf{R})$ given by

$$E_{ij}(\mathbf{R}) = -\sum_{kk'} |V_{k'i}|^2 |V_{kj}|^2 e^{-i(\mathbf{k}-\mathbf{k}')\cdot\mathbf{R}} F(\varepsilon_k, \varepsilon_{k'}) \qquad (2.4)$$

where $F(\varepsilon,\varepsilon')$ is given in Eq. (2.8) of Ref. 1. The sum in Eq. (2.4) involves contributions from bands above and below the Fermi energy and is free of divergences.

To apply Eq. (2.3) to the magnetic behavior of Pu compounds, matrix elements of H_{12} are taken in a basis restricted to members of the ground-state manifold of Pu.[10] The resulting expression for the two-ion exchange interaction in Pu compounds contains two factors: matrix elements of the one-electron creation and annihilation operators between ionic states ("scattering coefficients"), which contain all the information concerning the composition of the Pu ionic states, and the coefficients of the one electron transitions, the range parameters [Eq. (2.4)]. The details of the calculation of the scattering coefficients may be found in Refs. 10–13.

In the rocksalt structure Pu compounds, the range functions contain 28 independent components for each neighbor shell, and insight is necessary in the phenomenological theory to keep the number of independent parameters to a manageable level. In the Ce monopnictides, the dominant elements of the range function matrix are $E_{\pm 1/2,\pm 1/2}$ with one-electron states $|j=5/2,m_j\rangle$ quantized along the interionic axis, a result expected from the asymptotic ($k_F R \to \infty$) form of the range functions for free-electron bands.[8] The anisotropy in the magnetic behavior of CeSb results from the dominance of these components of the range functions: the selection rule $m_j, m_j' = \pm\frac{1}{2}$ favors the accumulation of charge along the interionic axis, and the tendency for CeSb to order with moments along a cube edge may be understood on the basis of this anisotropic interaction between ions placed in the cubic rocksalt environment.

Based on the success of the theory for the Ce monopnictides, the phenomenological theory for Pu systems adopted similar selection rules. Two scattering channels are currently incorporated into the phenomenological calculations: transitions for which $m_l = 0$ and $m_s = \pm\frac{1}{2}$, and transitions for which $m_l = \pm 1$ and $m_s = \mp\frac{1}{2}$. The phenomenological treatment, with these selection rules, has had great success in describing the magnetic behavior of PuSb.[13] In Sec. IV we give a qualitative comparison of range functions calculated for PuSb with the results of the phenomenological calculations for that compound, and discuss the trends in calculated range functions between the Pu monopnictides and between PuSb and PuTe. We find, in general, that for PuSb, the calculated parameters are in accord with the asymptotic selection rule and that the magnitudes and signs of the range parameters fitted in the phenomenological treatment are in general agreement with the corresponding components of the calculated range function matrices. We also find a marked change in the character of the range functions between PuSb and PuTe.

III. CALCULATION OF THE MODEL HAMILTONIAN PARAMETERS

The calculation of the parameters entering the Anderson model Hamiltonian for Pu compounds is quite similar to that for the Ce monopnictides, described in Ref. 1; the difference between the two calculations is in the treatment of the Pu $5f$ core states compared to the $4f$ core state in Ce. The reference system of the model Hamiltonian is the zeroth-order term in the Anderson Hamiltonian; i.e., Pu $5f$ states localized on Pu sites uncoupled to band states. Hence as the initial step for calculating the model Hamiltonian parameters, we calculate a self-consistent potential for each compound with Pu f states treated as core states, uncoupled to band states.

The electronic structure method used is a warped-muffin-tin LMTO method.[1] The bases of the band states are Bloch functions of muffin-tin orbitals centered on nonoverlapping muffin-tin spheres. The potential is spherically averaged within the muffin-tin spheres but has full spatial dependence in the interstitial region. Three energy panels are used, corresponding to the Pu $6p$ semicore states, anion s states, and valence states. The basis states have, in general, nonzero kinetic energy in the interstitial region; the interstitial kinetic energies of the bases are treated as variational parameters. The relative magnitudes of the muffin-tin radii are chosen so that nearest-neighbor muffin-tin spheres touch at the minimum in the charge density between nearest neighbors. While the basis functions for the band states are scalar relativistic,[18] spin-orbit coupling is included self-consistently.

The Pu f states are treated, self-consistently, as core states. Since the ground state of the Pu ion is close to the L-S coupled limit, we treat these states as scalar relativistic, rather than fully relativistic as was appropriate for Ce compounds.[1] Thus, while spin-orbit coupling is included in the band states, the spin-orbit interaction is neglected in calculating the Pu f states.

Treating the f states as localized (positive-energy) core states requires the imposition of a localization potential, or, equivalently, a boundary condition providing a square-integrable radial function. This boundary condition should be chosen so that the resulting charge density, a Pu $5f$ core, provides enough screening so that the band electrons see, as nearly as possible, a Pu^{3+} ion. In our calculations for the Ce monopnictides,[1] we defined a localized Ce f state by imposing a scattering resonance condition at the radius of the Ce muffin-tin sphere and a step-function barrier potential at a point greater than the muffin-tin radius to obtain a square integrable function. The f-state wave function obtained in this way was essentially identical, inside a Ce sphere, to that which we would have obtained had we treated the f states as itinerant, and the screening of the Ce ion by the f state was virtually complete, due to the extreme localization of the f-state charge density in the Ce monopnictides. The same boundary condition could be applied in defining the Pu $5f$ radial functions, but the greater spatial extent of the Pu $5f$ state, compared to the Ce $4f$ state, results in a significant, although not severe, loss of screening charge

density from the Pu muffin-tin sphere, and it is desirable to alter the boundary condition slightly to obtain a somewhat more tightly bound Pu $5f$ core.

For the purposes of the present calculation, a localized Pu $5f$ state is obtained as the solution of the scalar-relativistic radial equation,[18] for the potential within a Pu muffin-tin sphere, satisfying the boundary condition

$$\mathcal{D}\{\phi_f(\varepsilon,s)\} = -l-1 = -4 \ . \tag{3.1}$$

In Eq. (3.1), s is the radius of a Pu muffin tin sphere, $\mathcal{D}$ is the logarithmic derivative functional, and ϕ_f is the upper component of the $l=3$ radial wave function. The potential is taken to be zero outside the Pu sphere in calculating these states, hence the radial function satisfying Eq. (3.1) has algebraic decay $\propto r^{-4}$ outside a Pu sphere and satisfies the boundary condition of a "just bound" state of the Pu muffin-tin potential. The boundary condition, Eq. (3.1), is identical to that imposed in Ce systems in the limit $\varepsilon \rightarrow 0$, i.e., of being "just bound," and the choice of Eq. (3.1) in defining the Pu $5f$ core states is simply a device to obtain a somewhat more effective screening charge in the Pu muffin-tin core potential. With the boundary condition used in the present calculations, the $5f$ charge in a Pu sphere is about $4.9e$ for the compounds considered here. With the boundary condition used in the previous calculations[1] for cerium compounds, this charge would be only $\sim 4.75e$.

The electronic structure calculation provides us with a self-consistent potential with which we may calculate the band energies and band-f matrix elements entering the model Hamiltonian. During the self-consistency process, the muffin-tin energy parameters and the kinetic energies of the basis states in the interstitial are set to energies averaged over the occupied states. The bands of interest for the calculation of the model Hamiltonian parameters are those in the vicinity of the Fermi energy, derived mainly from Pu d-states and anion p states. To obtain an accurate description of these bands, we therefore perform a final band-structure calculation with the muffin-tin energy parameters of these basis states set at the band centers and the kinetic energy of the LMTO tails set equal to the Fermi energy. The resulting bands and band density of states are shown in Figs. 1–8 for PuAs, PuSb, PuBi, and PuTe.

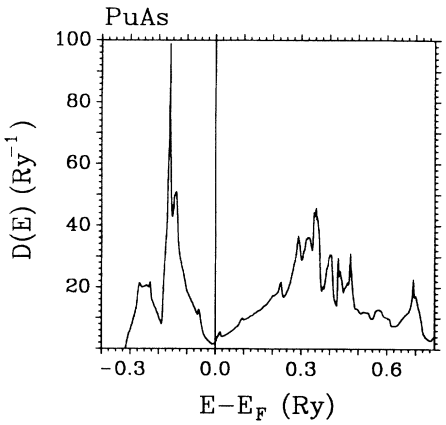

FIG. 2. The density of band states of PuAs corresponding to the band structure shown in Fig. 1.

This final step provides band energies as input to the model Hamiltonian, and band eigenvectors which we may combine with the Pu f-state wave functions and the self-consistent Pu muffin-tin potential to calculate the band-f hybridization matrix elements in the model Hamiltonian. As in the calculation for the Ce monopnictides, we make the approximation that all of the band-f mixing occurs within the Pu muffin tin. Projecting out band-f nonorthogonality,[1] we obtain the band-f matrix elements as

$$V(k,m_l m_s) = v(E_F) T^*(m_l m_s;k) \ , \tag{3.2}$$

where $T(m_l m_s,k)$ is a product of the LMTO band eigenvectors and the Korringa-Kohn-Rostoker structure function matrix. In Eq. (3.2), k represents both wave number and band index. The hybridization potential $v(E_F)$ in

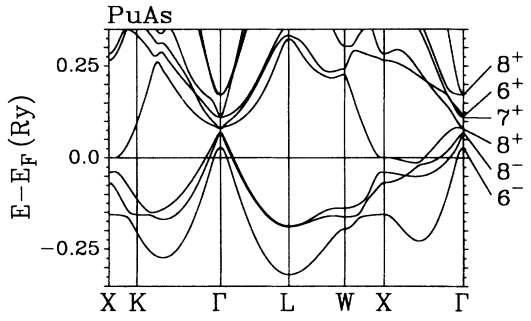

FIG. 1. The band structure of PuAs, calculated with the Pu $5f$ states treated as core states, along symmetry lines in the Brillouin zone. Energies (in Ry) are with respect to the Fermi energy. The labels on the right of the figure denote the symmetry of the bands at Γ. Bands with Γ_6^+ symmetry are derived from Pu $7s$ states, bands with Γ_6^- or Γ_8^- symmetry are derived from As $4p$ states, and bands with Γ_7^+ or Γ_8^+ symmetry are derived from Pu $6d$ states.

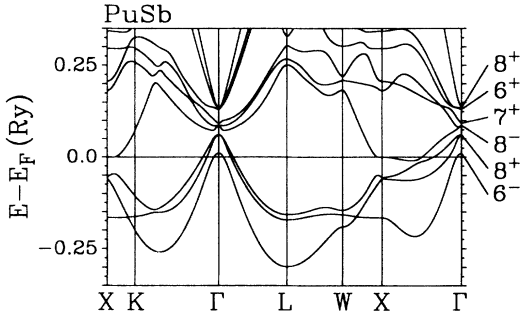

FIG. 3. The band structure of PuSb, calculated with the Pu $5f$ states treated as core states, along symmetry lines in the Brillouin zone. Energies (in Ry) are with respect to the Fermi energy. The labels on the right of the figure denote the symmetry of the bands at Γ. Bands with Γ_6^+ symmetry are derived from Pu $7s$ states, bands with Γ_6^- or Γ_8^- symmetry are derived from Sb $4p$ states, and bands with Γ_7^+ or Γ_8^+ symmetry are derived from Pu $6d$ states.

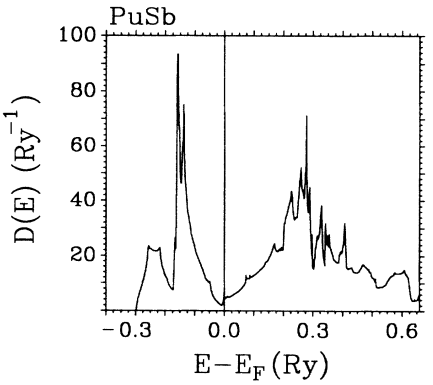

FIG. 4. The density of band states of PuSb corresponding to the band structure shown in Fig. 3.

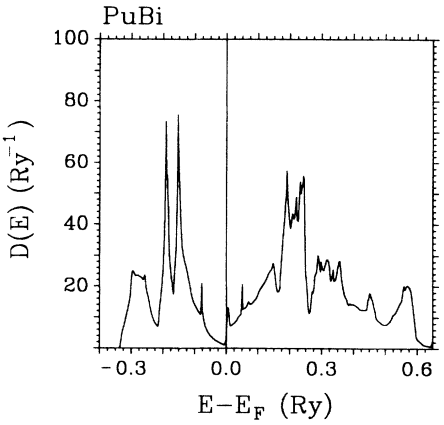

FIG. 6. The density of band states of PuBi corresponding to the band structure shown in Fig. 5.

Eq. (3.2) is given by

$$v(E_F)\approx -\left[\frac{\Gamma}{2k_F\Omega}\right]^{1/2}, \tag{3.3}$$

where n is a spherical Neumann function and s is the ranance width Γ is given by

$$\Gamma=\frac{2}{k_F}\left[\frac{\phi_f(s)}{n_3(k_Fs)}\right]^2 \tag{3.4}$$

where n is a spherical Neumann function and s is the radius of the Pu muffin-tin sphere.

The hybridization matrix element defined through Eq. (3.2) consists of an overall scale factor, $v(E_F)$, which varies for different compounds but is the same for all bands in a given compound, and the expansion coefficient of the tail of a band state expanded in spherical waves around a Pu site. From Eqs. (2.2) and (2.4) we see that the shift in the crystal-field levels is proportional to the resonance width Γ, and the range parameters are proportional to Γ^2. In Sec. IV we will use the resonance widths to gauge the relative strength of band-f hybridization for different Pu compounds. Equally important in characterizing the effects of hybridization between band states and Pu f states is the magnitude and character of the density of states at the Fermi energy. Calculated resonance widths and densities of state at E_F are given in Table I.

The final ingredients we require are the energies E_f and E_f+U to remove an electron from or add an electron to the Pu f^5 manifold. We obtain these from two self-consistent supercell calculations for PuSb (with a supercell equal to four unit cells), with the method described above but with one less or one more electron added to one of the four Pu sites in the supercell. We compare the resulting f-state eigenvalues with the eigenvalues resulting from the initial calculation and obtain linear transition state estimates for energies to remove or add a $5f$ electron.[15] We find $E_F-E_f=2.01$ eV and $E_f+U-E_F=1.97$ eV ($U=3.97$ eV) for PuSb.

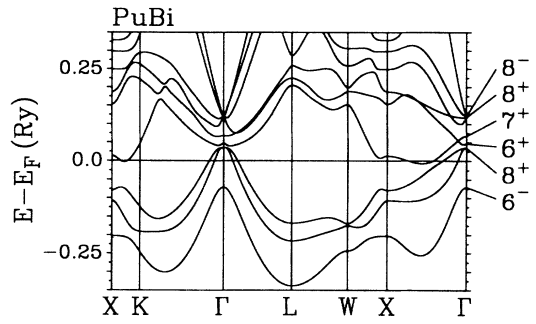

FIG. 5. The band structure of PuBi, calculated with the Pu $5f$ states treated as core states, along symmetry lines in the Brillouin zone. Energies (in Ry) are with respect to the Fermi energy. The labels on the right of the figure denote the symmetry of the bands at Γ. Bands with Γ_6^+ symmetry are derived from Pu $7s$ states, bands with Γ_6^- or Γ_8^- symmetry are derived from Bi $4p$ states, and bands with Γ_7^+ or Γ_8^+ symmetry are derived from Pu $6d$ states.

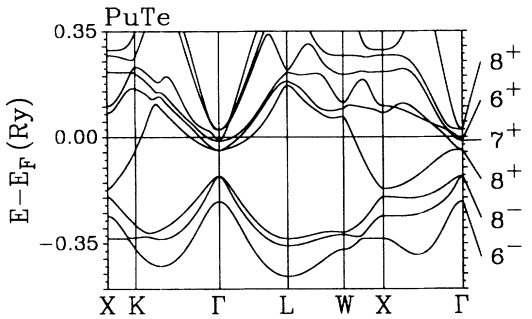

FIG. 7. The band structure of PuTe, calculated with the Pu $5f$ states treated as core states, along symmetry lines in the Brillouin zone. Energies (in Ry) are with respect to the Fermi energy. The labels on the right of the figure denote the symmetry of the bands at Γ. Bands with Γ_6^+ symmetry are derived from Pu $7s$ states, bands with Γ_6^- or Γ_8^- symmetry are derived from Te $4p$ states, and bands with Γ_7^+ or Γ_8^+ symmetry are derived from Pu $6d$ states.

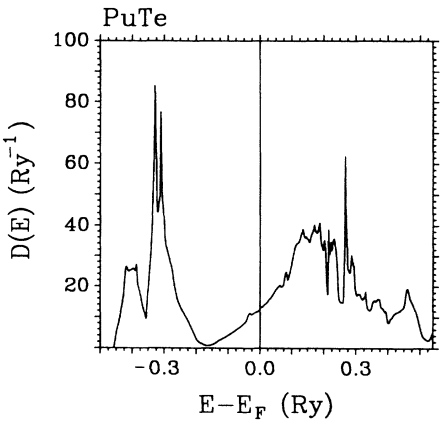

FIG. 8. The density of band states of PuTe corresponding to the band structure shown in Fig. 7.

IV. CRYSTAL-FIELD ENERGIES AND RANGE PARAMETERS

With the parameters entering the Anderson Hamiltonian calculated as in Sec. III, we may evaluate the quantities entering the model Hamiltonian for Pu compounds. The k-dependent quantities ε_k and $V(k,m_l m_s)$ are evaluated on a tetrahedral mesh in the irreducible part of the fcc Brillouin zone; integrals over the Brillouin zone are evaluated using the method of Gilat and Bharatiya.[19] Details of the numerical calculations are given in Ref. 1.

A. Crystal-field shift in PuSb

Evaluating the sum over band states in Eq. (2.1), we obtain a matrix which, when diagonalized, gives a shift in the one-electron f-state energy levels due to hybridization with band states, given by

$$E_{ij}^2 = \sum_k J_{ij}(k) \tag{4.1}$$

with $J_{ij}(k)$ given by Eq. (2.2). The bands entering the calculation of the matrix elements in Eq. (2.2) are spin-orbit coupled, hence the matrix E_{ij}^2 is diagonalized in a one-electron $|lsjm_j\rangle$ basis set. The relative shift in the crystal-field levels of the $j=\frac{5}{2}$ manifold for PuSb, defined by

$$\delta_{1e} = \Gamma_8(^2F_{5/2}) - \Gamma_7(^2F_{5/2}) \tag{4.2}$$

is shown in Table II. The one-electron Γ_8 level is lowered, relative to the Γ_7 level by 773 K. In the j-j coupled limit, the Pu ground-state manifold is a hole in the filled $j=\frac{5}{2}$ sextet; hence, in the limit of j-j coupling, we would conclude that the Γ_8 level of the Pu f^5 multiplet would be *raised,* relative to the Γ_7 level by 773 K. However, the ground state of the Pu ion is closer to the L-S coupled limit, being composed of $\approx 80\%$ $^6H_{5/2}$ character.[11-13]

To calculate the shift in the crystal-field levels in the L-S coupled limit, the f^5 $^6H_{5/2}$ states are decomposed into a sum over products of one-electron states and parent f^4 states; and we then obtain the matrix elements of H_2 [Eq. (2.1)] in the $^6H_{5/2}$ bases as a sum of products of one-electron matrix elements E_{ij}^2, Wigner coefficients, and fractional parentage coefficients.[20] The relative shift of the crystal-field levels of the $^6H_{5/2}$ sextet, defined by

$$\delta_{L\text{-}S} = \Gamma_8(^6H_{5/2}) - \Gamma_7(^6H_{5/2}) \tag{4.3}$$

is shown in Table II. For PuSb, the Γ_8 level is lowered, relative to the Γ_7 level by 193 K. To estimate the total splitting (the "bare" crystal field plus hybridization dressing) of the crystal-field levels, we assume that the environment of a Pu ion in a PuSb crystal is similar to that of Ce in a CeSb crystal. Using an effective anion charge of $Z=-1.2$, appropriate to CeSb,[21] and matrix elements $\langle r^4\rangle$ using Pu radial wave functions calculated as de-

TABLE I. Self-consistent electronic structure parameters for PuAs, PuSb, PuBi, and PuTe calculated as discussed in Sec. III. Γ is the full width of the $5f$ resonance in the self-consistent potential surrounding a Pu site, $\nu(E_F)$ is the single-site radial matrix element of the self-consistent potential surrounding a Pu site between the Pu $5f$ basis state and an $l=3$ spherical wave. $D(E_F)$ is the (non f) band density of states at the Fermi energy, $D_p(E_F)$ is the anion p projected density of states at the Fermi energy, and $D_d(E_F)$ is the Pu d projected density of states at the Fermi energy.

	Γ (mRy)	$\nu(E_F)$ (mRy)	$D(E_F)$ (Ry^{-1})	$D_p(E_F)$ (Ry^{-1})	$D_d(E_F)$ (Ry^{-1})
PuAs	8.89	−4.37	3.35	1.86	0.97
PuSb	6.14	−3.38	6.61	3.92	1.71
PuBi	7.26	−3.55	7.63	3.30	3.09
PuTe	12.19	−4.58	18.26	1.74	12.81

TABLE II. Relative shifts in the crystal-field levels due to hybridization between band states and f states, discussed in Sec. II and calculated as in Sec. IV for PuSb, PuAs, PuBi, and PuTe. δ_{1e} is the difference between the energy level shifts of the Γ_8 and Γ_7 one-electron $j=\frac{5}{2}$ Pu crystal-field f states, $\delta_{L\text{-}S}$ is the difference between the energy level shifts of the Γ_8 and Γ_7 states for the $^6H_{5/2}$ Pu f^5 multiplet. β/β_J is the ratio of the hybridization induced shift in crystal-field splitting of the $^6H_{5/2}$ multiplet to the induced shift in the absence of the spin-orbit interaction in the band states and with hybridization between band states and $j=\frac{7}{2}$ one-electron Pu f states set equal to zero. δ is an estimate of the total crystal-field splitting of the $^6H_{5/2}$ multiplet obtained by combining the hybridization induced shift with a point-charge model parametrized as discussed in Sec. IV. For $\delta_{L\text{-}S}$, negative numbers mean that the Γ_8 state is shifted downward relative to the Γ_7 state; for δ, negative numbers mean that the Γ_8 state is below the Γ_7 state.

	δ_{1e} (K)	$\delta_{L\text{-}S}$ (K)	β/β_J	δ (K)
PuAs	−1169	−276	0.599	−84
PuSb	−773	−193	0.634	−53
PuBi	−641	−157	0.623	−29
PuTe	−277	−15	0.137	+157

scribed in Sec. III, we obtain an estimate of 140 K as the bare crystal-field splitting ($\Gamma_8-\Gamma_7$) of the $^6H_{5/2}$ sextet. Combining this with the hybridization induced shift gives a total crystal-field splitting of -53 K (Γ_8 below Γ_7) for PuSb. Without experimental measurements yielding the "bare" (unhybridized) crystal-field levels such as exist for the cerium monopnictides in comparison to heavier rare-earth monopnictides,[21] or alternatively an *ab initio* calculation of the bare crystal-field splitting, this number should be regarded as a good estimate of the calculated net crystal-field splitting including hybridization. However, considering the uncertainties involved in the phenomenological evaluation[13] that we use to connect to experiment, the quality of this estimate is sufficient to test our treatment of the hybridization effects.

While we cannot give absolute significance to this final number, it is indicative of a reversal in sign of the crystal-field splitting from that expected without significant hybridization between band states and f states. There is as yet no directly measured experimental number with which we may compare this result, but the experimental evidence is that the Γ_8 level is lower than the Γ_7 level,[14] and this also comes out of the analysis involved in the phenomenological theory. The model Hamiltonian calculations of the magnetic excitation behavior[13] of PuSb, which treat the sign and magnitude of the crystal field as a fitted parameter, indicate that the Γ_8-Γ_7 splitting is on the order of -250 K. Considering the complexity of both the phenomenological theory[13] and of the present *ab initio* calculations, we regard the agreement with the present *ab initio* prediction as satisfactory, where we attach significance to the fact that we have been able to correctly predict the change in behavior from CeSb to PuSb with the Γ_8 level being driven below the Γ_7 level.

The quantity β/β_J, given in the third column of Table II, provides a measure of the importance of the spin-orbit effects within the bands in changing the calculated hybridization shift of the crystal-field levels. As discussed in Sec. IV, the departure of β/β_J from unity indicates the significance of such effects.

B. Range parameters of PuSb

As discussed in Sec. II, in order to keep the set of independent range parameters to a manageable size, certain selection rules have been used in the model Hamiltonian treatment of the Pu monopnictides, adopted from the theory for the Ce monopnictides.[8] The selection rules currently used in the model Hamiltonian calculations are $m_l=0$, $m_s=\pm\frac{1}{2}$ and $m_l=\pm1$, $m_s=\mp\frac{1}{2}$ (referenced to f states quantized along the interionic axis). These selection rules correspond to the asymptotic selection rules that would obtain if the coupling between f states on different ions were mediated by free-electron bands.[8] We have calculated the first, second, and third neighbor range function matrices [Eq. (2.4)] for PuSb in a one-electron $|lsjm_j\rangle$ basis with f states quantized along the interionic axes, and we find that the asymptotic selection rules of the phenomenological treatment are well justified. Of the twenty eight independent components, per neighbor shell, of the range function matrices, for all three neighbors we find that the components corresponding to $j=\frac{7}{2}\rightleftarrows j=\frac{7}{2}$ and $j=\frac{7}{2}\rightleftarrows j=\frac{5}{2}$ have a magnitude on the order of one percent of the magnitude of the components corresponding to $j=\frac{5}{2}\rightleftarrows j=\frac{5}{2}$. Within the subset of range functions corresponding to transitions within the $j=\frac{5}{2}$ manifold, while none of these components are negligible, they are dominated by the single component corresponding to $m_j=\pm\frac{1}{2}\rightleftarrows m_j=\pm\frac{1}{2}$. The magnitude of this component is a factor of 1.5 greater than the next largest component.

A fully quantitative comparison between calculated and phenomenological range parameters is not particularly illuminating. The phenomenological treatment isolates the dominant components of the range functions and fits them to the magnetic behavior of PuSb assuming all other components are zero. While it would seem that transitions within the $j=\frac{7}{2}$ manifold and transitions between the $j=\frac{7}{2}$ and $j=\frac{5}{2}$ manifolds may be safely neglected for treating PuSb, a quantitative assessment of the calculated range functions would still require comparing three fitted parameters per neighbor shell to six calculated parameters per neighbor shell (the independent components of the $j=\frac{5}{2}$ manifold), and we would not expect a detailed quantitative correspondence to obtain. A quantitative judgement of the calculated range functions must therefore be withheld until the full set of range functions can be accommodated in the phenomenological calculations.

In order to give a qualitative assessment of the calculated range functions and to show changes in the range functions on going to different Pu compounds, the component of the calculated range function matrices corresponding to $m_j=\pm\frac{1}{2}\rightleftarrows m_j=\pm\frac{1}{2}$ is given in Table III for the first-, second-, and third-neighbor shells of PuSb, PuAs, PuBi, and PuTe. A few qualitative conclusions may be drawn by comparing the component of the $j=\frac{5}{2}$ range functions listed in Table III for PuSb with parameters used in the model Hamiltonian calculations. In the phenomenological calculations[13] for PuSb, the nearest-neighbor range parameter corresponding to that given in Table III is related to the Néel temperature (85 K in PuSb), and, when this parameter is fit to the ordered states of PuSb, the result is generally larger in magnitude than the magnitude of the calculated parameter by a factor of 2 to 3. On this basis, we expect that the calculated range functions should predict a lower Néel temperature than is observed experimentally. The calculated ratio of second neighbor–to–first-neighbor range parameters is larger than the value generally used in the phenomenological calculations by a factor of about 3; however, the phenomenology[8,11–13] is not particularly sensitive to this ratio so long as the second-neighbor parameter is not much smaller than the first-neighbor parameter, and has the same sign, and we may say that the calculated ratio is consistent with the phenomenology. Both of the calculated first- and second-neighbor range parameters are ferromagnetic, again in agreement with the model Hamiltonian calculations. The calculated ratio of third-neighbor to nearest-neighbor range parameters is about

TABLE III. Calculated range parameters corresponding to the transition channels with $|m_j| = \frac{1}{2}$, defined in Sec. II and calculated as discussed in Sec. IV, for first, second, and third nearest neighbors in PuAs, PuSb, PuBi, and PuTe. The sign convention for the range parameters is such that $E_i < 0$ gives a ferromagnetic coupling.

	$j=\frac{5}{2}$			$j=\frac{7}{2}$		
	E_1 (K)	E_2/E_1	E_3/E_1	E_1 (K)	E_2/E_1	E_3/E_1
PuAs	−210	3.29	−0.01	−35	3.34	0.09
PuSb	−48	3.38	0.38	−1.4	1.13	0.38
PuBi	−77	2.69	0.09	−0.77	2.69	0.72
PuTe	−24	0.08	0.05	−11	0.22	0.22

the same as, but opposite in sign to, that usually used in the phenomenology; since, for third-neighbor interactions, this component ($m_j = \pm\frac{1}{2} \rightleftarrows m_j = \pm\frac{1}{2}$) does not dominate the $j=\frac{5}{2}$ submatrix of the range functions, it is difficult to assess the importance of this difference. On the basis of this comparison, we conclude that the calculated range functions, although possibly smaller in scale, are in qualitative agreement with the phenomenology. However, we reiterate that a quantitative assessment of the validity of our calculated *ab initio* range functions cannot be made until the full set of range function components can be incorporated into the phenomenological model Hamiltonian calculations for comparison with experiment, enabling us to have a fully defined comparison with the phenomenological theory and hence with experiment.

C. Trends between compounds

To conclude this section, we will discuss trends in the calculated crystal-field dressing and range parameters between PuSb and the neighboring Pu monopnictides, and between PuSb and PuTe, and analyze the source, in the electronic structure of these materials, of differences in the calculated quantities. For the purpose of analyzing hybridization effects within the context of our procedure for calculating Anderson model Hamiltonian parameters, band-f hybridization in these compounds may be approximately characterized by two quantities arising from our band-structure calculations: f-state resonance widths, characterizing the strength of hybridization, and the density of states at the Fermi energy, characterizing the number and character of band states available for hybridization. These quantities are listed in Table I.

In the pnictogen column, the resonance width is minimized at PuSb; a similar trend occurs in the Ce monopnictides.[1] On this basis, PuSb would be characterized as the Pu monopnictide in which band-f hybridization is weakest. The increase in the resonance width on moving up the column from PuSb to PuAs is approximately twice the increase on moving down the column to PuBi. It is interesting that, just as for the cerium monopnictides, the lattice parameters for the lighter monopnictides (PuAs and PuSb in the present work) are of a size that just accommodates Pu and pnictogen ions of "typical solid-state size," while the PuBi lattice parameter is too small to do this. Thus, while the increase of hybridization on going up the pnictogen column from the antimonide seems to have a very simple explanation in the naturally occurring decreased separation, and hence increased mixing between cerium ions, the increase in hybridization on going to the bismuthide comes from the effect of the lattice not expanding sufficiently, and hence the bismuth and plutonium ions being "squeezed" together. On moving from PuSb to PuTe, the resonance width increases by a factor of 2; the resonance width in PuTe is considerably larger than in any of the Pu monopnictides for which these calculations have been performed. On this basis, band-f hybridization in the Pu chalcogenides would seem to be much greater than in the Pu monopnictides.

The density of states at the Fermi energy, $D(E_F)$, increases going down the pnictogen column. $D(E_F)$ increases by a factor ≈ 2 from PuAs to PuSb; the increase from PuSb to PuBi is much less. In all the Pu monopnictides (Figs. 1–6), the Fermi energy lies in a gap between bands of predominantly pnictogen p character and Pu d character. In PuAs and PuSb, the pnictogen p-projected density of states, $D_p(E_F)$, is greater than the Pu d-projected density of states, $D_d(E_F)$ by approximately a factor of 2; in PuBi, $D_p(E_F)/D_d(E_F) \approx 1$. In PuTe, the Fermi energy lies at the bottom end of the Pu d bands, and the $D(E_F)$ in PuTe is greater than in PuSb by a factor of approximately 3; for PuTe, $D_p(E_F)/D_d(E_F) = 0.14$.

On the basis of the large resonance width and $D(E_F)$ in PuTe, relative to the Pu monopnictides, the effects of band-f hybridization in PuTe might be expected to be much stronger than in the Pu monopnictides. Thus it is striking that the quantities we have applied our calculations to, the crystal-field dressing and range parameters, are smaller in PuTe than in the Pu monopnictide. Comparing the results of the calculations for PuTe and the Pu monopnictides, shown in Table II, it is evident that the relative shift in the crystal-field levels in PuTe is much less than in the Pu monopnictides. Both the one-electron shift and the shift in the ${}^6H_{5/2}f^5$ states are significantly less than the corresponding shifts for the Pu monopnictides. The reason for this sharp decrease in the calculated crystal-field dressing in PuTe, despite the larger hybridization strength and density of states at the Fermi energy, is that the shift [Eq. (2.1)] in the one-electron levels is the result of two competing effects. The contribution from bands above the Fermi energy is negative, while the contribution from bands below the Fermi energy is positive. Bands just above the Fermi energy in the Pu monopnictides that give a strong negative contribution to the shift in the crystal-field energies fall just below the Fermi energy in PuTe, and their contribution is reversed in sign.

A smaller contribution to the difference between the one-electron shifts in the Pu monopnictides and in PuTe arises from the change in the character of the bands near the Fermi energy. Pnictogen (or chalcogen) derived p states hybridize more strongly with Pu f states because the Pu-anion separation is smaller than the Pu-Pu separa-

tion. In the Pu monopnictides, the bands just above the Fermi energy have a mixture of p and d character, while in PuTe, the p character is negligible. However, in both cases hybridization involving d band states just above the Fermi energy dominates the f crystal-field shift. As discussed in Ref. 1, the lowering of the Γ_8 relative to the Γ_7 crystal-field level is essentially caused by the greater multiplicity of the Γ_8.

The change in the character of the density of states near the Fermi energy may be an important factor in the resulting negligible suppression of the crystal-field states of the ${}^6H_{5/2}$ multiplet in PuTe shown in Table II. The third column of Table II (β/β_J) gives the ratio of the calculated shift in the crystal-field splitting of the ${}^6H_{5/2}$ multiplet to the shift that would result from the one-electron shifts given in the first column of Table II if the spin-orbit splitting of the band states were absent and if the band states did not hybridize with one-electron $j=\frac{7}{2}$ f states. This ratio is much smaller in PuTe than in the Pu monopnictides. The spin-orbit interaction is more important for bands of Pu d character than for the anion p bands, and hence the change in the character of the density of states near the Fermi energy in PuTe may be responsible for the negligible effect on the ${}^6H_{5/2}$ multiplet.

The components of the range function matrices corresponding to the phenomenological range parameters are shown in Table III for PuAs, PuSb, PuBi, and PuTe. For the reasons stated in Sec. IV B, we will not speculate on details of the trends in magnetic behavior to be expected on the basis of the results shown in Table III without the necessary refinement of the phenomenological theory. There are, however, several qualitative differences in calculated range parameters between the Pu monopnictides and PuTe which we wish to note. The magnitude of the first-neighbor parameter, E_1, which sets the scale of the magnetic interaction in the phenomenological calculations, is much smaller in PuTe than in the Pu monopnictides, and we would expect a much smaller Néel temperature on this basis. It is also evident in Table III that the decrease in the magnitude of the range parameters is much more rapid with increasing neighbor distance than in the Pu monopnictides, indicating a short-range magnetic interaction. In particular, the ratio of second- to first-neighbor parameters, which relates to the size of the zero-temperature moment in the phenomenological calculations,[8] is negligible in PuTe, compared with the Pu monopnictides. It is also evident, from the results given in Table III, that hybridization between band states and one-electron $j=\frac{7}{2}$ f states will have much greater importance in PuTe than in the Pu monopnictides. Beyond these detailed comments, however, we should emphasize that the striking change in the magnitude and character of the range parameters calculated for PuTe, compared to those calculated for the Pu monopnictides, indicates *a qualitative change in the nature of the magnetic behavior that would be predicted on the basis of the calculations presented here.* Indeed such a qualitative change in behavior compared to PuSb is indicated at a more primitive level in the theory by the jumps in Γ and $D(E_F)$ shown in Table I, by factors of 2 and 3, respectively. Thus we might expect a strong qualitative change in the basic nature of the magnetic behavior such as we have treated for the change from CeSb to CeTe (Ref. 22) but even stronger. For CeTe, we believe that the strong decrease in magnetic ordering (decrease in Néel temperature and ordered moment by an order of magnitude from CeSb is associated with CeTe experimentally being an incipient heavy fermion). The stronger changes in Γ and $D(E_F)$ from PuSb to PuTe compared to those on going from CeSb to CeTe, might lead us to anticipate a transition to a truly different type of electronic magnetic behavior. It is therefore striking that experimentally PuTe shows no magnetic ordering, but enhanced Pauli paramagnetism, and is thought to be a heavy-fermion system. Thus, the greatest value of our *ab initio* calculations of range parameters for the plutonium compounds is in predicting trends within and between families of isostructural compounds and in signaling a transition to a wholly different regime of behavior such as the heavy-fermion or valence fluctuation regimes of behavior. Furthermore, besides giving a signal of such a transition, the present theory allows us to recognize the features in the underlying electronic structure driving such a transition.

V. SUMMARY

In this paper we have presented a scheme for obtaining Anderson model Hamiltonian parameters for Pu compounds from first-principles band-structure calculations for Pu monopnictides and PuTe. In order to make contact with experiment and phenomenological calculations, the results have been applied to the calculation of two quantities arising in a model Hamiltonian theory of weakly hybridizing Pu systems: a shift in the crystal-field levels of the Pu ion and the coefficients of the hybridization-induced exchange interaction between Pu ions. Calculations for PuSb have been compared with experiment and phenomenology. The calculated crystal-field is in qualitative agreement with the behavior previously deduced[13] by a phenomenological treatment of the magnetic equilibrium and excitation behavior in which parameters were evaluated by considering experimental behavior. For the calculated range parameters of the two-ion exchange interaction, the conclusion we may draw at present is that the results of the present *ab initio* calculations are highly promising with regard to comparison with the existing phenomenological results, and await extension and refinement of the phenomenological theory to enable a detailed quantitative comparison. The agreement of the calculated quantities with available experimental and phenomenological results is similar to the agreement obtained in a previously reported calculation of the same quantities for the Ce monopnictides. The most striking result of the present calculations is to lead us to anticipate experimental behavior for PuTe very strongly differing from that of PuSb. Experimentally, there is a change to heavy fermion behavior.[23–26]

The results of our calculations of the hybridization induced crystal-field shift suggest that the total effective crystal field in these Pu compounds is opposite in sign to that in the corresponding Ce compounds; i.e., the hybrid-

ization shift is strong enough to drive the Γ_8 level below the Γ_7 level. The validity of our results, and hence of our physical picture and methodology is supported by such behavior experimentally in PuSb.[14] The band-structure method which we have used in these calculations makes a spherical approximation to the potential within muffin tins, and, while this approximation is appropriate for CeSb and CeBi where the effective crystal field is close to zero,[1] including nonspherical components of the potential may be important in calculations for the Pu compounds we have considered here; and the use of the warped-muffin-tin approximation, rather than using a full potential including the exact potential within the muffin-tin spheres, may be a significant deficiency in the present calculations for a fully quantitative evaluation of the crystal-field effects.

As discussed by us in Ref. 1 in connection with the calculations for the cerium compounds, from the computational point of view, three factors determine the sensitivity of the present calculations: the accuracy of the self-consistent potential, the size of the mesh in the Brillouin zone providing the eigenvalues and eigenvectors for the analyses, and the energies E_f and $E_f + U$ with respect to the Fermi energy. The treatment of the k mesh and quality of convergence are as discussed in Ref. 1. As in that case, the potential and total energy are converged to within ~ 0.3 mRy.

Two quantities arising in the calculation of the model Hamiltonian parameters, the f-state resonance width and the density of band states at the Fermi energy, show that the band-f hybridization is considerably stronger in PuTe than in the Pu monopnictides. A possible consequence of this result is that the neglect of higher-order terms in the Schrieffer-Wolff transformation of Anderson Hamiltonian, which is appropriate in the limit of weak hybridization, and gives rise to the expressions [Eqs. (2.1) and (2.3)] for the crystal-field shift and the exchange interaction, may not be appropriate for the more strongly hybridizing compound PuTe. Hence, while the Anderson Hamiltonian parameters which we calculate may be applicable to this compound, the expressions for the crystal-field shift and two-ion exchange interaction may not be. If we assume that the neglect of higher-order terms is still a meaningful approximation, a second point arises as a consequence of stronger hybridization in PuTe: it may be that nonlinear effects (the self-consistent determination of the bands and f states in the presence of band-f hybridization in the context of the model Hamiltonian) may have a significant effect on results of the calculations presented here. Thus while the present *ab initio* calculations are adequate to signal a transition to a different state of magnetic behavior for PuTe compared to PuSb or the other stable magnetically ordered systems, we cannot expect it to describe what in fact experimentally is a heavy-fermion state.

With regard to comparing our *ab initio* calculations of range parameters with the phenomenological (model Hamiltonian) evaluation of Ref. 13, the reader should bear in mind that because the Pu^{3+} has five f electrons rather than the single f electron of the Ce^{3+} ion, the phenomenological theory for the plutonium compounds is of necessity more complex than that for the cerium compounds. As briefly described in Sec. II above, this complication is treated in Ref. 13 by introducing a hierarchy of scattering channels in the context of a resonant-scattering-type theory, and including only what on a physical basis are regarded as the dominant channels. This introduces an additional level of uncertainty in relating the phenomenological theory with experiment and into relating our present *ab initio* calculations with the phenomenological results.

Finally, we want to emphasize that our primary objective in this work has been to establish the applicability of the methodology we have developed, including necessary refinements on going from cerium in Ref. 1 to plutonium here, to systematically understand and predict similarities and changes in hybridization dominated electronic and magnetic behavior on going from the single-f-electron cerium systems to the relatively more delocalized five-f-electron plutonium systems. Thus our focus is on treating the utility and success of the methodology for predicting and understanding the systematics of hybridization-dominated observational behavior associated with changes in the underlying electronic structure and degree of f-electron delocalization. For this reason we focus our attention on the systematics of calculationally predicted changes of behavior for isostructural materials, e.g., changes going down the pnictogen column for cerium or plutonium monopnictides, or on going from a pnictide to the adjacent chalcogenide (e.g., antimonide to telluride), or on the changes from a cerium compound to the corresponding plutonium compound. We believe that we have been quite successful in demonstrating the suitability of the methodology for attacking these systematics with the most striking success being the signal of something importantly different about PuTe compared to PuSb. We also recognize and plan to attack the need for further refinements and improvements while centering on the desire to understand effects of increased hybridization or delocalization as distinct from the technical complications introduced to treat the intraionic correlation effects for the many-f-electron ion.

ACKNOWLEDGMENTS

The work at Los Alamos National Laboratory has been supported by the U.S. Department of Energy and that at West Virginia University by the National Science Foundation through Grant No. DMR-88-07523.

[1] J. M. Wills and B. R. Cooper, Phys. Rev. B **36**, 3809 (1987).

[2] Proceedings of Actinides 85 Conference, Aix En Provence, France, edited by M. Beuvy (Elsevier Sequoia, Lausanne, 1986), *ACTINIDES 85*, (also appeared as Vol. 121 of the Journal of the Less-Common Metals).

[3] P. Burlet, S. Quezel, J. Rossat-Mignod, J. C. Spirlet, J. Rebizant, W. Muller, and O. Vogt, Phys. Rev. B **30**, 6660 (1984).

[4] G. H. Lander, W. G. Stirling, J. Rossat-Mignod, J. C. Spirlet,

J. Rebizant, and O. Vogt, Physica **136B**, 409 (1986).
[5]D. J. Lam and A. T. Aldred, *The Actinides: Electronic Structure and Related Properties,* edited by A. J. Freeman and J. A. Darby, Jr. (Academic, New York, 1974), Vol. 1, Chap. 3, pp. 109-179; K. Mattenberger, O. Vogt, J. C. Spirlet, and J. Rebizant, J. Less-Common Met. **121**, 285 (1986); G. H. Lander, J. Rebizant, J. C. Spirlet, A. Delapalme, P. J. Brown, O. Vogt, and K. Mattenberger, Physica **146B**, 341 (1987).
[6]B. R. Cooper, P. Thayamballi, J. C. Spirlet, W. Mueller, and O. Voigt, Phys. Rev. Lett. **51**, 2418 (1983).
[7]B. Coqblin and J. R. Schrieffer, Phys. Rev. **185**, 847 (1969).
[8]B. R. Cooper, R. Siemann, D. Yang, P. Thayamballi, and A. Banerjea, in *The Handbook on the Physics and Chemistry of the Actinides,* edited by A. J. Freeman and G. H. Lander (North-Holland, Amsterdam, 1985), Vol. 2, Chap. 6, pp. 435–500.
[9]J. L. Smith and Z. Fisk, J. Appl. Phys. **53**, 7883 (1982).
[10]P. Thayamballi and B. R. Cooper, J. Appl. Phys. **55**, 1829 (1984).
[11]A. Banerjea, B. R. Cooper, and P. Thayamballi, Phys. Rev. B **30**, 2671 (1984).
[12]A. Banerjea and B. R. Cooper, Phys. Rev. B **34**, 1607 (1986).
[13]G.-J. Hu, N. Kioussis, A. Banerjea, and B. R. Cooper, Phys. Rev. B **38**, 2639 (1988).
[14]G. H. Lander, A. Delapalme, P. J. Brown, J. C. Spirlet, J. Rebizant, and O. Vogt, Phys. Rev. Lett. **53**, 2262 (1984); J. Appl. Phys. **57**, 3748 (1985).
[15]M. R. Norman, D. D. Koelling, A. J. Freeman, H. J. F. Jansen, B. I. Min, T. Oguchi, and Ling Ye, Phys. Rev. Lett. **53**, 1673 (1984).
[16]J. R. Schrieffer and P. A. Wolff, Phys. Rev. **149**, 491 (1966).
[17]B. Cornut and B. Coqblin, Phys. Rev. B **5**, 4541 (1972).
[18]D. D. Koelling and B. N. Harmon, J. Phys. C **10**, 3107 (1977).
[19]G. Gilat and N. R. Bharatiya, Phys. Rev. B **12**, 3479 (1975).
[20]B. R. Judd, *Operator Techniques In Atomic Spectroscopy* (McGraw-Hill, New York, 1963).
[21]R. J. Birgeneau, E. Bucher, J. P. Maita, L. Passell, and K. C. Turberfield, Phys. Rev. B **8**, 5345 (1973).
[22]N. Kioussis, B. R. Cooper, and J. M. Wills, J. Appl. Phys. **63**, 3683 (1988).
[23]B. R. Cooper, J. M. Wills, N. Kioussis, and Q. G. Sheng, J. Appl. Phys. **64**, 5587 (1988).
[24]K. Mattenberger, O. Vogt, J. C. Spirlet, and J. Rebizant, J. Less-Common Met. **121**, 285 (1986).
[25]J. M. Collard, A. Blaise, J. M. Fournier, and J. P. Charvillat, J. Less-Common Met. **121**, 223 (1986).
[26]P. G. Therond, A. Blaise, J. M. Fournier, J. Rossat-Mignod, J. C. Spirlet, J. Rebizant, and O. Vogt, J. Magn. Magn. Mater. **63**, 142 (1987).